Journal of Materials Chemistry A

Accepted Manuscript

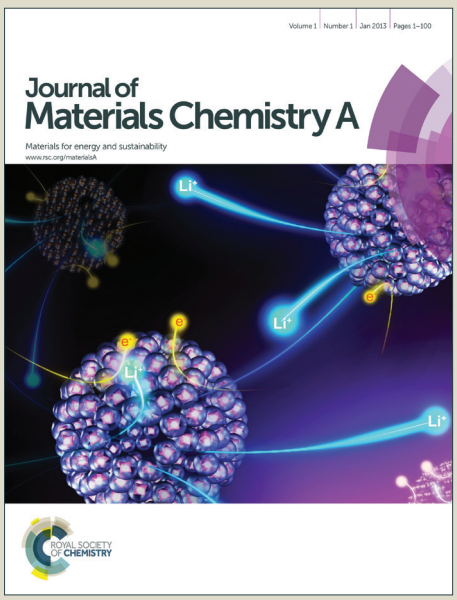

ROYAL SOCIETY OF CHEMISTRY

www.rsc.org/materialsA

Journal Name

RSCPublishing

ARTICLE

Magnetic Ni and Ni/Pt hollow nanospheres and their catalytic activities for hydrolysis of ammonia borane

Cite this: DOI: 10.1039/x0xx00000x

Wenliang Jiao, Xiaopeng Hu, Hao Ren, Pengfei Xu, Ranbo Yu*, Jun Chen, and Xianran Xing

Received 00th January 2012,
Accepted 00th January 2012

DOI: 10.1039/x0xx00000x

www.rsc.org/

Hollow metallic nickel nanospheres have been controllably synthesized via a solvothermal reduction process. The complexation between ethylenediamine and Ni^{2+} might be the key factor to control the formation of the hollow structure through the reduction rate of Ni^{2+} at a relatively low level. The size of the hollow nanospheres could be adjusted by changing the starting ethanol/ethylenediamine molar ratio. The magnetic properties study reveals that the coercivity of the as-synthesized hollow nickel nanospheres is much enhanced comparing with that of bulk nickel materials. Ni/Pt hollow bimetallic nanospheres have also been synthesized by using replacement reaction. Inspiringly, the as-synthesized Ni/Pt hollow bimetallic nanospheres exhibit higher catalytic activities for the hydrogen generation from ammonia borane hydrolysis compared with the Ni/Pt nanoparticles.

Introduction

Hydrogen is considered one of the best alternative energy carriers, because of its clean and environmentally friendly properties[1] and high-energy content equal to 142 MJ/kg[2]. Controlled storage and release of hydrogen are the most challenging technologies to realize the hydrogen in commercial use. Up to now, a great deal of work has been done to develop effective hydrogen storage materials to satisfy the hydrogen fuel cell and other hydrogen energy systems[3]. Owing to its high hydrogen content of 19.6% (3 mol H_2 per mol ammonia borane), nontoxicity and high stability, ammonia borane (AB) has been considered one of the most promising candidates for the chemical hydrogen-storage applications[4-8]. The release of hydrogen from AB could be obtained by hydrolysis[9], catalytic dehydrogenation in nonaqueous solvent[10] and thermal decomposition[11]. With appropriate catalyst AB can conveniently hydrolyze and release hydrogen at room temperature[12]. Among all the catalysts, nickel-based one is promising in the future, because of its low cost and resource rich[13]. Therefore, considerable attention has been focused on developing of new type of nanostructured nickel and nickel based catalysts[14].

As the superior catalysts, nickel materials were designed into special nanoscale structures and morphologies, such as nanoparticles[4], nanowires[15], nanotubes[16] et al, since different structures and morphologies might lead to different physical and chemical performance of materials[17]. Nanostructured hollow sphere[18] attracted more and more attention in recent years, because of its special structures and unique properties. For example, the void space in hollow structure has been used to improve the particles' ability to withstand cyclic change in volume[19], modulate refractive index[20], increase active area for catalysis and encapsulate the sensitive materials (e.g. drugs, cosmetics and DNA)[21]. As for nickel-based catalyst, endowing hollow structure with it may also lead to improvement in its performance in wide areas, so the corresponding synthesis attracted more attention in recent years. The template method is the most versatile way to fabricate nickel and nickel-based hollow spheres. By using this approach, hollow Ni submicrometer spheres and nickel silicate composite were successfully prepared[22-24]. However, the products with these methods are often difficult to purify, and usually the procedures are tedious. Thus, template-free methods were also explored. For example, hollow nickel spheres were successfully synthesized via a decomposition and reduction route[25], and porous hollow nickel microspheres were synthesized by self-assembly in an aqueous medium[26]. Apparently, the synthesis of hollow structured nickel material is mainly lie in the microscale, and related properties were rarely studied so far. Exploring systematic synthesis and developing novel approach to nanostructured hollow nickel spheres are still of great significance.

Herein, we demonstrate a solvothermal method for fabricating hollow nickel nanospheres. The as-synthesized hollow nickel nanospheres can be obtained without any further processing. On the basis of replacement reaction, Ni/Pt hollow nanospheres have also been synthesized with the hollow nickel nanospheres as sacrificial templates. The magnetic properties of nickel hollow nanospheres and the dehydrogenation activities of Ni/Pt hollow sphere were investigated. It is found that the as-synthesized Ni/Pt hollow nanospheres exhibit high catalytic activities for the hydrolysis of AB at room temperature.

Experimental

All chemicals used in this experiment were analytical grade (purchased from Beijing Chemical Co. Ltd) and used without any further purification.

Preparation of hollow Ni nanospheres. The growth of the hollow nanospheres was carried out in a solution system. $NiCl_2 \cdot 6H_2O$ was firstly dried in a vacuum oven to remove the water of crystallization. 0.23 g of obtained $NiCl_2$ was dissolved in a 30mL of ethanol/ethylenediamine mixed solution with certain volume ratios (1:9, 3:7, 4:6, 5:5) under intensive stirring for 1h. Then, 0.12 g of $NaBH_4$ was introduced to the solution followed with another intensive stirring for 5min. Afterward, the as-prepared solution was transferred to a Teflon-line stainless-steel autoclave, and maintained at 150°C for 6 h. The black solid product was collected by centrifuging and sequentially rinsed with ethanol and deionized water for several times. The final product was dried in a vacuum oven at 50°C for 6h.

Preparation of Ni/Pt hollow bimetallic nanospheres. The as-prepared hollow nickel nanospheres were suspended in deionized water by ultrasonic treatment, followed by adding a freshly prepared HCl solution (5 wt%) to remove the oxidation layer on the surface of hollow nickel nanospheres. The freshly obtained hollow nickel nanospheres were suspended in deionized water again with ultrasonic treatment. Afterward, newly prepared K_2PtCl_6 solution (3.6mM, 5ml, 10.5ml, 16.7ml, corresponding to the Ni/Pt molar ratio of 95:5, 90:10, 85:15) was added to the suspension drop by drop with mechanical stirring. Finally, the Ni/Pt hollow nanospheres were collected by centrifugation, washed with deionized water and then dried in a vacuum oven at 50 °C for 6h.

Characterization. The obtained samples were characterized on a Panaltical X' Pert-pro MPD X-ray powder diffractometer (XRD) with Cu Kα radiation (λ=1.5418Å).The operation voltage and current were kept at 40kV and 40mA, respectively. The transmission microscope (TEM) and the corresponding selected area diffraction (SAED) and high-resolution TEM (HRTEM) were obtained on a JEOL JEM-2100 microscope operated at an acceleration voltage of 200kV. The scanning electron microscopy (SEM) images were taken on a LEO 1530 scanning electron microscope. The magnetic properties were investigated with a superconducting quantum interference device (SQUID-VSM) magnetometer.

Catalytic hydrogen generation from AB hydrolysis. The hydrolysis of AB was carried out at room temperature. In a typical process, a 10mg of Ni (or Ni/Pt) hollow nanospheres was first dispersed in 10 mL of deionized water with ultrasonic treatment, and 70 mg of AB was dissolved in 10 mL deionized water. Then, both the Ni (or Ni/Pt) suspension and the AB solution were mixed in a three-necked flask connecting with an inverted, water-filled graduated burette. During the reaction, constant stirring was applied. The volume of generated H_2 was recorded with corresponding time.

Results and discussion

Morphology and structure. Transmission electron microscope (TEM) was applied to analyze the structure of the as-synthesized hollow nickel nanospheres. Figure 1A, B, C, D shows the hollow nickel nanospheres obtained in different volume ratios of ethanol and ethylenediamine (ET/EN) at 150°C. As shown in the Figure 1A, we can hardly obtain any hollow nickel nanospheres at the ET/EN ratio of 1:9. When the ratio is higher than 1:9 as 3:7, 4:6, and 5:5, hollow nickel nanospheres with average diameter of 170nm, 260nm, and 450 nm and average shell thickness of 55~60 nm (Figure 1B, C and D) were obtained. Obviously, with the increase of the ethanol amount, the size of the hollow spheres increases. At the ET/EN ratio of 4:6, the nickel hollow nanospheres are relatively uniform. When the ratio reaches 5:5, the uniformity of nickel hollow nanospheres become worse, and lots of large nickel particles were also formed. These results indicate that the ratio of ET/EN plays a key role to control the size and uniformity of the nickel hollow nanospheres.

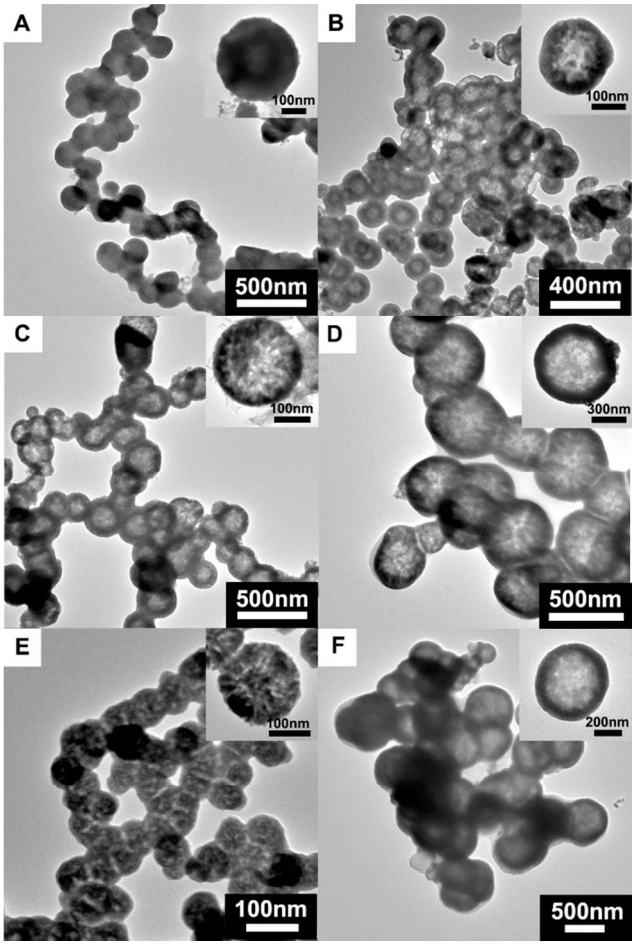

Figure 1 TEM images of the as-synthesized nickel hollow nanospheres at different ratios of ET/EN and temperatures. (A) ET/EN =1:9, (B) ET/EN =3:7, (C), ET/EN =4:6, (D) ET/EN =5:5, (E) 120°C, (F) 180°C.

Temperature affected the nickel hollow spheres formation critically. Figure 1E, F show the products synthesized at 120°C and 180°C with the ET/EN ratio of 4:6. With the comparison of Figure 1C, it can be seen that, with the increase of the synthetic temperature, the obtained final products follow the similar trend as the ratio of ET/EN. Higher temperature affects the complexation reaction equilibrium, which will lead to the increase of reduction rate. At the lower temperature of 120°C, uniform nickel spheres without obvious shell were obtained. While at higher temperature of 180°C, besides the formation of Ni hollow spheres, the seriously aggregated Ni particles can also be formed, and the diameter of the nickel hollow spheres were also increased. Thus, we can conclude that the ET/EN ratio of 4:6 and the heating temperature of 150°C are the optimum conditions for the synthesis of nickel hollow nanospheres.

To further confirm the phase purity of the hollow Ni nanospheres, we collected their XRD patterns. There are three characteristic peaks with 2θ values of 44.5, 51.8, 76.4, which well match the (111), (200), (220) of face centered cubic (fcc) nickel. It can also be seen that no other peaks are observed except the peaks of nickel. It shows the well crystallinity and high purity of the obtained nickel hollow nanospheres. Based on the XRD pattern, the size of the crystal nanoparticles were calculated by using Scherrer equation, which shows the average size of the crystallized nanoparticles is 25nm~30nm. Moreover, the sample was investigated by selected area electron diffraction (SAED). The diffraction pattern exhibited a remarkable polycrystalline feature as shown in Figure 2B. Three ring patterns corresponding to the indices 111, 200, 220 of fcc nickel were assigned in the image. Figure 2C shows the high-resolution TEM (HRTEM) of the nickel hollow nanospheres. The lattice plane spacings measured from the HRTEM image is 0.20 nm, which is close to the (111) interplanar distance of fcc nickel structure (0.203 nm).

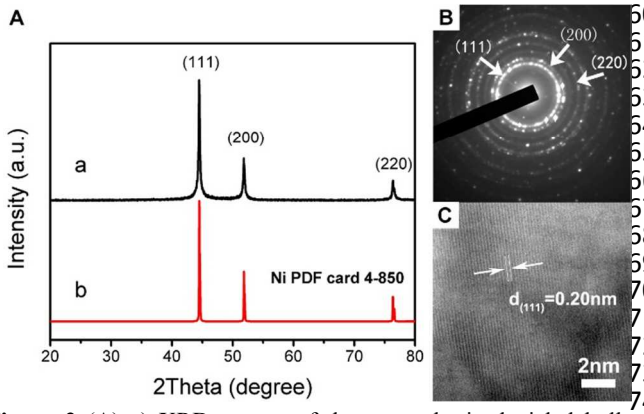

Figure 2 (A) a) XRD pattern of the as-synthesized nickel hollow spheres, b) the nickel PDF card 4-850. (B) SAED image of the as-synthesized nickel hollow nanospheres. (C) HRTEM image of the as-synthesized nickel hollow spheres.

According to previous literatures[27 28] and the above results in the present study, we believe that the ethanol, ethylenediamine and synthesis temperature play important roles in the formation of the nickel hollow nanospheres. The ethanol in the precursor solution may act as a bridge to resolve and deliver the free Ni^{2+}, thus the free Ni^{2+} can be reduced to metallic nickel by $NaBH_4$. With the increase of the ratio of ethanol, the reaction rate tends to become faster. It is reasonable to interpret the formation process using the assembly-then-inside-out evacuation mechanism[29], as shown in Figure 3.

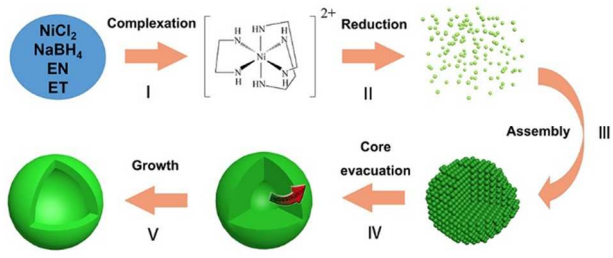

Figure 3 Schematic illustration of the formation and shape evolution of hollow nickel metallic nanospheres in the whole synthetic process.

In the beginning (I), Ni^{2+} cations in the solution reacted with excess ethylenediamine (EN) to form a relatively stable structure of $[Ni(EN)_3]^{2+}$ complex[30], which cannot be reduced by $NaBH_4$ directly. Due to the formation of the $[Ni(EN)_3]^{2+}$ complex, the concentration of the free Ni^{2+} in the solution sharply decrease. Afterward, under a proper solvothermal condition, these $[Ni(EN)_3]^{2+}$ complex could decompose and release free Ni^{2+} to the solution at a low rate, which was then reduced to small nickel nanoparticles (II).

The chemical reactions involved in the preparation process are described as:

$$Ni^{2+} + 3[EN] \leftrightarrow [Ni(EN)_3]^{2+} \quad (1)$$

$$Ni^{2+} + BH_4^- + 2H_2O \rightarrow Ni\downarrow + BO_2^- + 2H^+ + 3H_2\uparrow \quad (2)$$

Due to the controlled releasing of the free Ni^{2+}, the reduction rate can be controlled at a relatively slow level that can effectively prevent the formation of large nickel particles. According to the minimization of interfacial energy[31] and the magnetic dipole-dipole interaction, the newly formed nickel nanoparticles are unstable and tend to aggregate with each other to form larger nickel spheres (III). With more Ni^{2+} reduced, the subsequent reduced nickel grows on the surface of the nickel spheres, leading to the formation of a new type of nickel spheres, which is composed of small nanoparticles in the core and large nanoparticles on the surface. Furthermore, the small nanoparticles in the core of these nickel spheres resolved (IV), possibly through a mechanism of Ostwald ripening. As the solvothermal time was prolonged, more interior nanoparticles resolved, and the interior hollow space became larger and larger (V), thus formed the final hollow nickel nanospheres. Based on the formation mechanism and the role of ethanol in the reaction, we may modulate the size of the nickel hollow spheres by adjusting the ratio of ET/EN and the heating time. More ethanol amount means stronger deliver function in the reaction, which may lead to the formation of bigger nickel hollow spheres. Prolonging the heating time will also promote the formation of bigger nickel hollow spheres.

Magnetic properties. The magnetic properties of as-synthesized hollow nickel nanospheres were characterized by both magnetic field dependence of magnetization and temperature dependence of magnetization, zero-field-cooling (ZFC) and field-cooling (FC). Hysteresis loops were measured at 2K and 300K respectively, as shown in Figure 4A. The magnetic saturation reached with the external field exceeding 7.5 kOe. It shows that the saturation magnetization (M_s), remanent magnetization (M_r), and coercivity (H_c) are ca. 28.10emu g^{-1}, 8.13 emu g^{-1}, and 255 Oe respectively, at 2K and ca. 23.38 emu g^{-1}, 4.02 emu g^{-1}, 252 Oe respectively, at 300K. Compared with the H_c value of bulk nickel (ca. 0.7 Oe) and that of submicrometer-sized hollow nickel spheres (32.3 Oe) at room temperature[19], the as-synthesized hollow nanospheres exhibited much enhanced coercivity. In the ZFC mode, the test sample was cooled from room temperature to 2K without any external magnetic field. Then, a magnetic field of 90 Oe was applied, and the sample was measured during the warming process. In the FC mode, the test sample was cooled from room temperature to 2K under an external magnetic field of 10 kOe, and the sample was measured during the warming process under a constant magnetic field of 90 Oe. The ZFC and FC curves are shown in Figure 4B. The behavior of M(T) curves reveals the main feature of thermal activation effect against of the anisotropy barrier[32]. We can see a small peak in the $M_{ZFC}(T)$ at about 14K, which is identified as the frozen moment in the surface layer of particles. The similar behavior has been

observed in the nickel nanoparticles chains by assembly of small nanoparticles[33].

Ni/Pt hollow bimetallic nanospheres. Platinum is one of the best catalysts for many catalytic reactions. Due to the hollow structure nature of the as-synthesized nickel spheres, it can be set as a very good noble metal carrier. Herein, platinum growing on the surface of nickel hollow spheres well separate on the shell of nickel hollow spheres, which can increase the active sites of the platinum on the surface of the nickel hollow spheres during the catalytic reaction. In

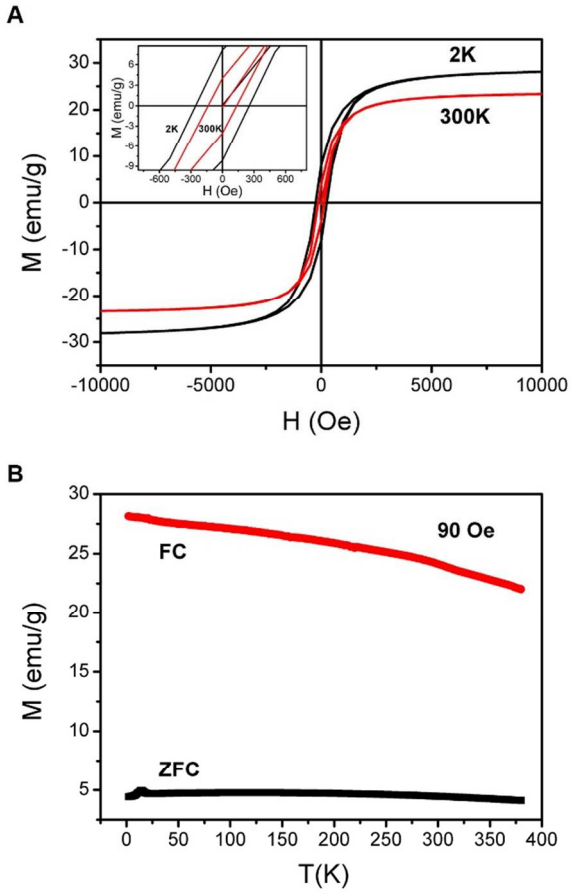

Figure 4 Hysteresis loops and FC ZFC curves of the as-synthesized hollow nickel nanospheres (A) Hysteresis loops of the as-synthesized hollow nickel nanospheres at 2K and 300K. The inset is the enlargement of the center part of the curves. (B) FC and ZFC curves of the as-synthesized hollow nickel nanospheres.

this work, the Ni/Pt hollow bimetallic nanospheres were synthesized through replacement reaction by using the as-synthesized hollow nickel nanospheres as sacrificial temple. The driving force of the replacement reaction comes from the large standard reduction potential gap between the Ni^{2+}/Ni redox pair (-0.25 V vs standard hydrogen electrode (SHE)) and the $PtCl_6^{2-}$/Pt redox pair (0.74 V vs SHE)[22 25].The molar ratio of nickel and platinum can be controlled by adding certain amount of K_2PtCl_6 solution. Herein, the hollow spheres with Ni/Pt molar ratio of 95:5, 90:10 and 85:15 were synthesized. The elemental composition was investigated by EDAX, which shows the average molar ratios of the as-synthesized Ni/Pt hollow spheres match well with the design. Figure 5A shows the

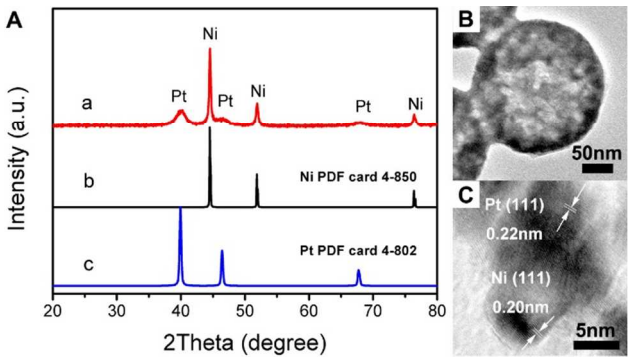

Figure 5 (A) a) XRD pattern of as-synthesized Ni/Pt hollow bimetallic nanospheres, b) the nickel PDF card 4-850, c) platinum PDF card 4-802. (B) TEM image of single as-synthesized Ni/Pt hollow bimetallic nanosphere. (C) HRTEM image of as-synthesized Ni/Pt hollow bimetallic nanospheres.

XRD pattern of as-synthesized Ni/Pt hollow bimetallic spheres, where both nickel and platinum exist as elementary substance. On the other hand, the TEM images of Ni/Pt hollow nanospheres (Figure 5B, Figure S3) indicate that upon loading of Pt, the morphology of the Ni hollow spheres does not change. The average diameter and wall thickness of the Ni/Pt hollow bimetallic nanospheres is 250nm and 40~55nm respectively. In the HRTEM image (Figure 5C), the lattice plane spacing of Ni (111) and Pt (111) could be detected clearly at the same time. Thus we can conclude that the platinum nanoparticles are distributed on the surface of nickel hollow spheres.

Catalyst properties. As a promising catalyst hydrogen carrier in the future, AB is stable in air and aqueous solution at room temperature. With the catalysis over proper catalyst, 1 molar of AB can release 3 molar hydrogen. The chemical reactions of the hydrolysis of AB can be described as follows:

$$NH_3BH_3 + 2H_2O \rightarrow NH_4^+ + BO_2^- + 3H_2 \uparrow \quad (3)$$

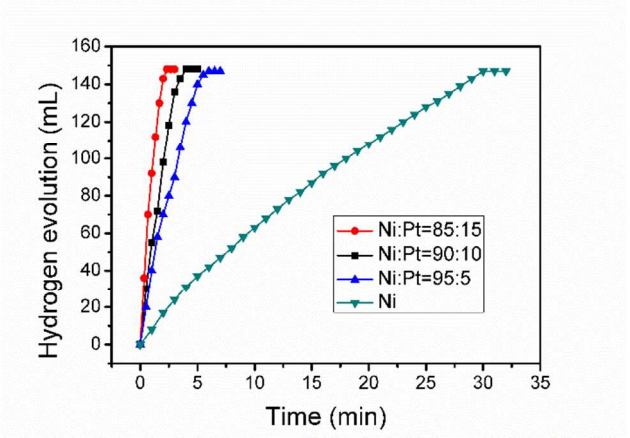

Figure 6 Hydrogen generation from the hydrolysis of aqueous ammonia borane solution (AB, 200Mm, 20mL) catalyzed by Ni and Ni/Pt hollow nanospheres at room temperature.

Figure 6 shows the hydrogen release from AB catalyzed by as-synthesized Ni hollow nanospheres and Ni/Pt hollow bimetallic nanospheres with three different percentages composition (the molar ratio of Ni/Pt, 95:5, 90:10, 85:15). We can see that the pure nickel

hollow nanospheres exhibit relatively low catalytic activity for hydrolysis of AB at room temperature, while the as-synthesized Ni/Pt hollow bimetallic nanospheres greatly increase the hydrolysis rate of AB. Of all the three Ni/Pt hollow bimetallic nanospheres samples, the sample with the molar ratio of 85:15 exhibits the fast catalytic rate, with which the reaction is completed within only 3 min. The rate of hydrogen generation on the molar ratio of Ni/Pt hollow bimetallic nanospheres attains 5920 mL min^{-1} g^{-1}, which is higher than that of ex situ synthesized $Ni_{0.81}$-$Pt_{0.19}$ nanoparticles (about 5251 mL min^{-1} g^{-1})[34]. We may conclude that the hollow structure benefit the catalytic reaction. Because of the nickel substrate with hollow structure, platinum on the nickel hollow spheres may have more opportunity to contact with AB in the solution, which is undoubtedly of benefit to the reaction kinetics.

Conclusions

In summary, a novel synthesis strategy has been demonstrated for the creation of hollow nickel nanospheres through a solvothermal method. Through the assembly-then-inside-out evacuation mechanism based on Ostwald ripening hollow nickel nanospheres with controlled sizes could be formed. The magnetic properties of as-synthesized hollow nickel nanospheres exhibited much enhanced coercivity comparing with its bulk and submicrometer hollow spherical counterparts. Ni/Pt hollow bimetallic nanospheres have also been obtained via a replacement reaction route by using hollow nickel nanospheres as sacrificial templates. The Ni/Pt hollow bimetallic nanospheres exhibited high catalytic activities for the hydrogen generation from AB hydrolysis at room temperature. Based on the catalytic and magnetic properties, the as-synthesized hollow spheres may find some applications in fuel-cell-based hydrogen economy and many other fields.

Acknowledgements

This work was financially supported by the National Natural Science Foundation of China (No. 51072020, 21271021, 21031005). Special thanks to Prof. Dan Wang (Institute of Process Engineering, Chinese Academy of Sciences, China) for his valuable discussion and worthful advice.

Notes and references

Department of Physical Chemistry, University of Science and Technology Beijing, Beijing 100083, PR China.
E-mail: ranboyu@ustb.edu.cn

† Electronic Supplementary Information (ESI) available: SEM images, XRD data, TEM image, TEM-EDAX, reusability of catalyst. See DOI: 10.1039/b000000x/

1 L. Schlapbach, A. Züttel, *Nature,* 2001, **414**, 353-358.
2 S. B. Kalidindi, M. Indirani, B. R. Jagirdar, *Inorg. Chem.,* 2008, **47**, 7424-7429.
3 L. Yang, W. Luo, G. Cheng, *ACS appl. Mater. Interfaces,* 2013, **5**, 8231-8240.
4 O. n. Metin, V. Mazumder, S. Ozkar, S. Sun, *J. Am. Chem. Soc.,* 2010, **132**, 1468-1469.
5 J.-M. Yan, X. B. Zhang, S. Han, H. Shioyama, Q. Xu, *Inorg. Chem.,* 2009, **48**, 7389-7393.
6 C. W. Yoon, L. G. Sneddon, *J. Am. Chem. Soc.,* 2006, **128**, 13992-13993.
7 Q. Xu, M. Chandra, *J. Power Sources,* 2006, **163**, 364-370.
8 M. Chandra, Q. Xu, *J. power sources,* 2006, **156**, 190-194.
9 F. Durap, M. Zahmakıran, S. Özkar, *Appl. Catal. A: Gen.,* 2009, **369**, 53-59.
10 N. Blaquiere, S. Diallo-Garcia, S. I. Gorelsky, D. A. Black, K. Fagnou, *J. Am. Chem. Soc.,* 2008, **130**, 14034-14035.
11 Z. Xiong, C. K. Yong, G. Wu, P. Chen, W. Shaw, A. Karkamkar, T. Autrey, M. O. Jones, S. R. Johnson, P. P. Edwards, *Nature Mater.,* 2008, **7**, 138-141.
12 H. Liang, G. Chen, S. Desinan, R. Rosei, F. Rosei, D. Ma, *Int. J. Hydrogen Energy,* 2012, **37**, 17921-17927.
13 M. Danilova, Z. Fedorova, V. Zaikovskii, A. Porsin, V. Kirillov, T. Krieger, *App. Catal. B: Env.,* 2014, **147**, 858-863.
14 H.-L. Jiang, Q. Xu, *Catal. Today,* 2011, **170**, 56-63.
15 A. K. Bentley, M. Farhoud, A. B. Ellis, A. M. L. Nickel, G. C. Lisensky, W. C. Crone, *J. Chem. Educ.,* 2005, **82**, 765.
16 F. Tao, M. Guan, Y. Jiang, J. Zhu, Z. Xu, Z. Xue, *Adv. Mater.,* 2006, **18**, 2161-2164.
17 Y. Sun, Y. Xia, *Science,* 2002, **298**, 2176-2179.
18 I. H. Chen, C. C. Wang, C. Y. Chen, *Scripta Materialia,* **2008**, **58**, 37-40.
19 S. Xu, C. M. Hessel, H. Ren, R. Yu, Q. Jin, M. Yang, H. Zhao, D. Wang, *Energy. Environ. Sci.,* 2014, **7**, 632-637.
20 Z. Dong, X. Lai, J. E. Halpert, N. Yang, L. Yi, J. Zhai, D. Wang, Z. Tang, L. Jiang, *Adv. Mater.,* 2012, **24**, 1046-1049.
21 X. W. Lou, L. A. Archer, Z. Yang, *Adv. Mater.,* 2008, **20**, 3987-4019.
22 F. Cheng, H. Ma, Y. Li, J. Chen, *Inorg. Chem.,* 2007, **46**, 788-794.
23 Y. Wang, C. Tang, Q. Deng, C. Liang, D. H. Ng, F. L. Kwong, H. Wang, W. Cai, L. Zhang, G. Wang, *Langmuir,* 2010, **26**, 14830-14834.
24 J.C. Bao, Y. Y. Liang, Z. Xu, L. Si, *Adv. Mater.,* 2003, **15**, 1832-1835.
25 R. Yi, R. Shi, G. Gao, N. Zhang, X. Cui, Y. He, X. Liu, *J. Phys. Chem. C,* 2009, **113**, 1222-1226.
26 Q. Zhu, Y. Zhang, J. Wang, F. Zhou, P. K. Chu, *Sol. State Sci.,* 2011, **13**, 438-443.
27 D.-E. Zhang, X. J. Zhang, X. M. Ni, H. G. Zheng, *Mater. Lett.,* 2006, **60**, 1915-1917.
28 D. Yu, X. Sun, J. Zou, Z. Wang, F. Wang, K. Tang, *J. Phys. Chem. B,* 2006, **110**, 21667-21671.
29 L. P. Zhu, H. M. Xiao, W. D. Zhang, G. Yang, S. Y. Fu, *Cryst. Growth Des.,* 2008, **8**, 957-963.
30 S. A. Reisinger, A. S. de Sousa, M. A. Fernandes, C. B. Perry, P. R. Varadwaj, H. M. Marques, *Inorg. Chem. Commun.,* 2010, **13**, 584-588.
31 C. Wu, Y. Xie, L. Lei, S. Hu, C. OuYang, *Adv. Mater.,* 2006, **18**, 1727-1732.
32 N. Wang, X. Cao, D. Kong, W. Chen, L. Guo, C. Chen, *J. Phys. Chem. C,* 2008, **112**, 6613-6619.
33 L. He, W. Zheng, W. Zhou, H. Du, C. Chen, L. Guo, *J. Phys-Condens. Mater.,* 2007, **19**, 036216.
34 J. Du, F. Cheng, M. Si, J. Liang, Z. Tao, J. Chen, *Int. J. Hydrogen Energy,* 2013, **38**, 5768-5774.

Graphical TOC

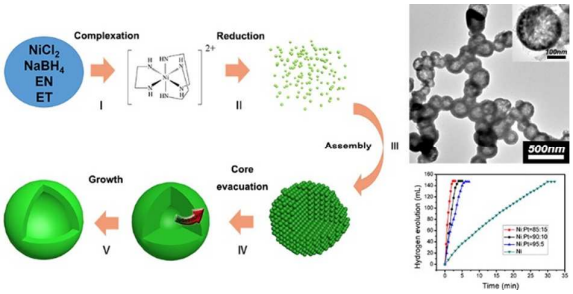

Controllable solvothermal synthesis of hollow nickel nanospheres were achieved via an assembly-then-inside-out evacuation process. The Ni/Pt hollow spheres exhibit high catalytic activities for the hydrolysis of ammonia borane.